Journal of the European Ceramic Society **11** (1993) 455–461

On the Correlation between Mechanical Damage and the Electrical Properties of Zirconia Ceramics

Azita Khalili

Max-Planck-Institut für Metallforschung, Institut für Werkstoffwissenschaft, Seestraße 92, D-W-7000 Stuttgart 1, Germany

&

Karl Kromp

Institut für Festkörperphysik, Universität Wien, Strudlhofgasse 4, A-1090 Vienna, Austria

(Received 13 July 1992; accepted 11 September 1992)

Abstract

This paper refers directly to a previous investigation, where Vickers indentations of different loads were applied to a YSZ-zirconia and then impedance spectroscopic parameters were measured in dependence on the indentation load. The aim of the present paper was to find a correlation between the impedance spectroscopic parameters and mechanical damage, e.g. microcracks. Stress intensity factors, K_c*, were evaluated by the ICL (indentation crack length) and ISB (indentation strength in bending) methods, to characterize the material mechanically, and were compared to* K_c *from conventional bending experiments with notched specimens. By SEM investigations of the as-indented surfaces and of the fracture surfaces after breaking open the specimens, the radial/median and the lateral crack systems were investigated. The observed crack systems could be correlated to the impedance spectroscopic parameters given in Ref. 1 and it is demonstrated that it is possible to characterize microcracks in ionic ceramics by impedance spectroscopy.*

Diese Arbeit bezieht sich auf eine frühere Veröffentlichung von L. Dessemond und M. Kleitz[1] *über den Einfluß mechanischer Schädigung auf die elektrischen Eigenschaften von Zirkoniumdioxidkeramiken. In diesen Untersuchungen wurden unter verschiedenen Lasten Vickers-Eindrücke in YSZ-Zirkoniumdioxid hergestellt, das als Modellwerkstoff für Ionen-leitende Keramiken verwendet wurde. Anschließend wurden die Impedanz-spektroskopischen Parameter als Funktion der Last bestimmt. Das Ziel der vorliegenden Arbeit ist die Klärung der Korrelation zwischen den Impendanz-spektroskopischen Parametern und der mechanischen Schädigung, z. B. Mikro-rissen. Um die mechanischen Eigenschaften des Materials zu charakterisieren, wurden die Spannungsintensitätsfaktoren* K_c *mittels der ICL (Indentation Crack Length) und der ISB (Indentation Strength in Bending) Methode bestimmt. Diese Ergebnisse wurden mit experimentellen* K_c*-Werten, die aus konventionellen Biegeversuchen an gekerbten Proben gewonnen wurden, verglichen. Durch rasterelektronenmikroskopische Untersuchungen der mit Eindrücken versehenen Proben und der Bruchflächen der durchgebrochenen Proben wurden die Systeme der radialen und der durchlaufenden Risse und das Quer-Rißsystem betrachtet. Die beobachteten Rißsysteme konnten mit den Impedanz-spektroskopischen Parametern, die in Ref. 1 angeführt werden, korreliert werden. Des weiteren wird gezeigt daß die Charakterisierung von Mikro-rissen in ionen-leitenden Keramiken durch Impedanz-Spektroskopie möglich ist.*

Cette communication se réfère directement à l'article 'Effects of mechanical damage on the electrical properties of zirconia Ceramics' de L. Dessemond et M. Kleitz.[1] *Dans cette recherche précédente, des indentations Vickers ont été réalisées sous différentes charges, sur de la zircone stabilisée à l'yttrium et utilisée comme modèle d'une céramique conductrice ionique; dès lors, les paramètres de spectroscopie d'impédance ont été mesurés en fonction de la charge. L'objectif du présent article est de trouver une corrélation entre les paramètres de spectroscopie d'impédance et les dommages mécaniques, par*

Journal of the European Ceramic Society 0955-2219/93/$6.00

exemple les micro-fissures. Le facteur d'intensité de contrainte, K_c, a été évalué par les méthodes ICL (mesure des fissures provoquée par indentation) et ISB (flexion d'éprouvettes indentées) afin de caractériser mécaniquement le matériau et les résultats ont été comparés au K_c mesuré par des essais de flexion conventionnels sur des éprouvettes entaillées. Des observations par MEB des surfaces indentées et des faciès de rupture des échantillons testés, ont permis d'étudier les réseaux de fissures radiales et médianes. Les réseaux de fissures observés pourraient être mis en corrélation avec les paramètres de spectroscopie d'impedance donnés en Ref. 1 et il est démontré qu'il est possible de caractériser les microfissures dans les céramiques ioniques par spectroscopie d'impédance.

1 Introduction

1.1 The Indentation Technique

In the past the indentation technique proved to be a useful tool, not only to characterize ceramic materials by hardness, but also to evaluate stress intensity factors K_c. Here indentation was used primarily to introduce defined damage to the ceramic material. Figure 1 shows the indentation fracture pattern of a Vickers indentation. The characteristic dimension of the 'plastic' indenter impression is half the diagonal of the indentation pattern under the peak load P and c is the characteristic dimension of the radial/median crack system. With the ICL method (indentation crack length) the length of the diagonal of the Vickers impression, $2a$, and the length of the surface radial cracks, c, are measured under the microscope. These parameters relate directly to the hardness H and the toughness K_c of the indented material:[2]

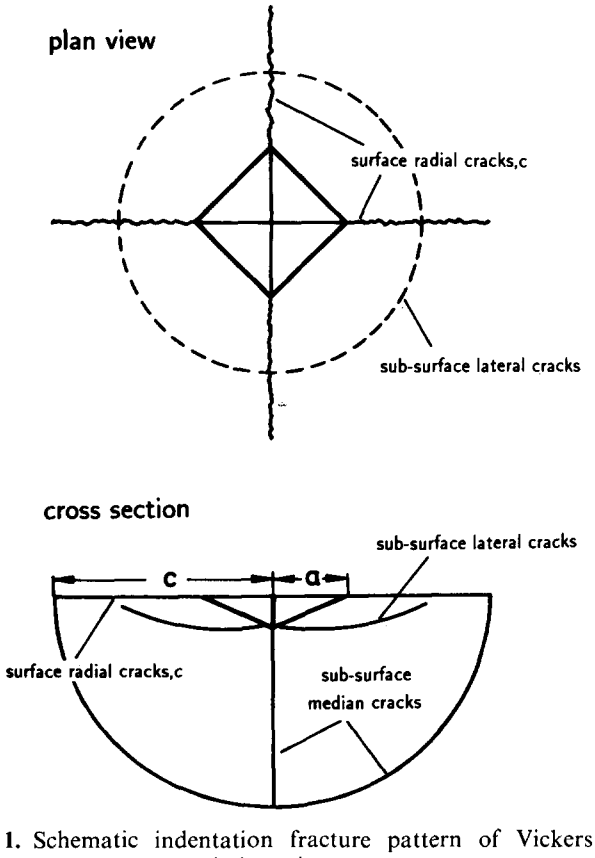

Fig. 1. Schematic indentation fracture pattern of Vickers indentation.

$$H = \frac{P}{\alpha_0 a^2} \tag{1}$$

$$K_c = \frac{P}{\beta_0 c^{3/2}} \tag{2}$$

where α_0 and β_0 are numerical constants. For Vickers indenters $\alpha_0 = 2$ if H is identified with the mean contact pressure. β_0 corresponds to a complex geometrical factor, for which here $1/\beta_0 = 0{\cdot}0824$ is taken from the standardized form, given by Ponton *et al.*[3]

The sub-surface lateral crack system spreads out from the deformation zone in the centre of the indentation pattern beneath the indentation surface and interacts with the radial/median system. There arise two superimposed components to the driving force on the crack system: an elastic (reversible) and a residual (irreversible) component.[4] At the indentation surface the elastic component is compressive and the residual component is tensile. The radial/median cracks grow to their final lengths when the indenter is unloaded, as the restraining elastic field is removed.

The lateral cracks tend to grow more extensively in post-indentation subcritical crack growth (influenced by surrounding media) until they ultimately catch up with the radial/median front. Usually the range of lateral cracks does not exceed that of radial/median cracks. In severely loaded specimens the lateral cracks turn upward to intersect the surface, thereby causing a disruption of the indentation pattern by chipping.

It is supposed that interactions between the lateral and the radial/median system influence the bending strength of a post-indentation bending test. The bending strength may increase because of a 'screening' of the radial/median system by the lateral cracks. The evaluation of K_c by eqn (2) involves the problem of not only measuring the diagonal $2a$ of the central impression, but also of measuring the radial crack length c.

In a post-indentation experiment using the ISB method (indentation strength in bending) the fracture strength is measured, where the indentation crack system is the critical starting defect. From the equation[5]

$$K_c = \eta_V^R \left(\frac{E}{H}\right)^{1/8} (\sigma P^{1/3})^{3/4} \tag{3}$$

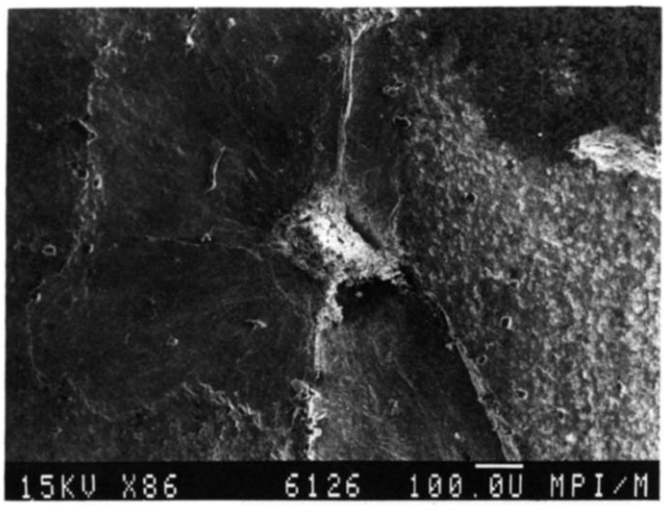

Fig. 2. Surface indentation pattern: radial cracks, crushing beneath the indenter, chipping (specimen 10, $P = 612{\cdot}5$ N).

where E is Young's modulus and σ is the bending strength, the toughness can be evaluated without measuring the crack length c. For a series of standard materials $\eta_V^R = 0{\cdot}59 \pm 0{\cdot}12$ was evaluated.[5] This method is based on a mechanical equilibrium crack length c_m, which reflects an invariance of η_V^R. Geometrical variations in the indentation pattern would result in a deviation of η_V^R, which means eqn (3) indirectly depends on crack length c via η_V^R.[5]

1.2 Material and starting point of the investigation

An yttria fully stabilized zirconia (YSZ) of around 95% of the theoretical density and an average grain size of 13 μm was investigated. The material of the system $(ZrO_2)_{1-x}(Y_2O_3)_x$ with $x = 0{\cdot}1$ (10 mol%) was prepared by wet mixing ZrO_2 and Y_2O_3 powders without sintering aid to avoid any chemical addition. The material was compacted at 200 MPa and sintered for 2 h in air at 1850°C.[1]

Prismatic specimens of a dimension $3 \times 7 \times 12\,mm^3$ were indented by Vickers indentation at different loads to introduce microcracks. Impedance spectroscopic investigations were then performed with these specimens,[1] because a potential application of impedance spectroscopy was to apply the method for the nondestructive detection of microcracks in ionically conducting materials.[1]

The impedance spectroscopic investigations were performed by placing a pinshaped platinum electrode near the indentation pattern and coating the rear surface of the specimen with a silver paste as a counter electrode. The pin was placed in the symmetry axis of the indentation pattern, 0·25 mm from one of the corners.

After the impedance spectroscopic measurements one batch of specimens, indented at nine different load levels, was further investigated electro-optically and mechanically, reported in the following, to find a correlation between the impedance spectroscopic data and the microcracks.

2 Experimental Investigations

The indentation patterns of the batch of specimens, loaded to different load levels (enumerated 2–10, number 1 being the as-received material without indentation) were photographed in the SEM at different magnifications. From these photographs the diagonals $2a$ of the central indentation and the length of the surface radial cracks were evaluated (see Fig. 2). To investigate the sub-surface median and lateral crack system, it was necessary to break the specimens at the indentation site. For this purpose a bending experiment was performed with the indentation pattern as the defect for brittle fracture. The original specimens were of the dimensions $3 \times 7 \times 12\,mm^3$, therefore the specimens had to be lengthened to load them at a span of 30 mm. This was achieved by glueing zirconia specimens of the same cross section to both ends of the specimens with Araldite. The specimens were then loaded to fracture in three-point bending at a stress rate of 35 MPa/s and a span of 30 mm. The specimens failed exactly at the indentation pattern, except specimen 3, which failed at a big structural defect (inclusion) near the indentation pattern (see Table 1). The Araldite layer was very thin, therefore

Table 1. Indentation pattern crack systems and the K_c values from ICL method for different loads

Specimen *Sp*	*Load* *P* (*N*)	*1/2 Diagonal* *a* (μm)	*Radial* *c* (μm)	*Lateral* (μm)	*Hardness* *H* (*GPa*)	*K_c from eqn (2)* K_c ($MPa\sqrt{m}$)
2	29·4	40	130	130	9·2	1·63
3	49	55	—	—	8·1	—
4	98	80	300	300	7·7	1·56
5	153·1	100	400	400	7·7	1·57
6	196	110	500	600	8·1	1·44
7	294	125	650	750	9·4	1·46
8	392	150	800	900	8·7	1·43
9	490	170	900	850	8·5	1·50
10	612·5	190	1 000	—	8·5	1·60
Mean values					$8{\cdot}43 \pm 0{\cdot}64$	$1{\cdot}52 \pm 0{\cdot}08$

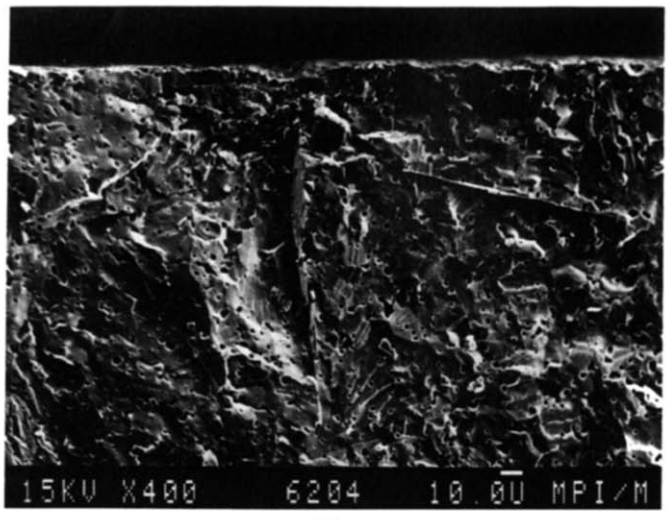

(a)

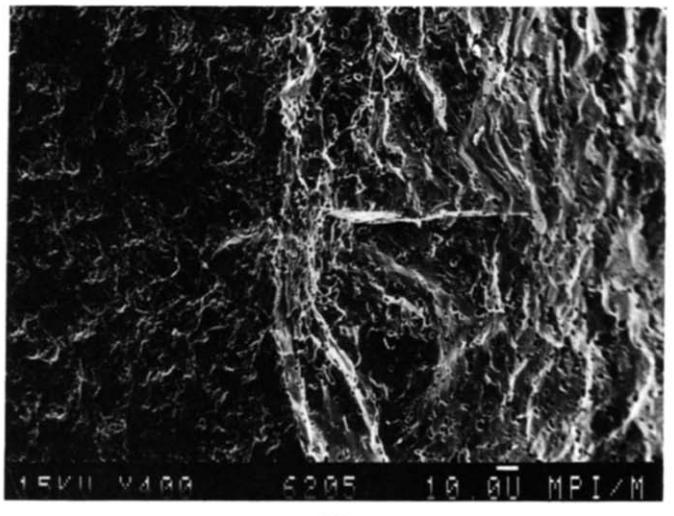

(b)

Fig. 3. Post-indentation fracture surfaces (specimen 2, $P = 29{\cdot}4$ N). (a) Crushing beneath the indenter, median and lateral cracks, (b) indentation pattern, median and lateral cracks at a tilt angle of 20°.

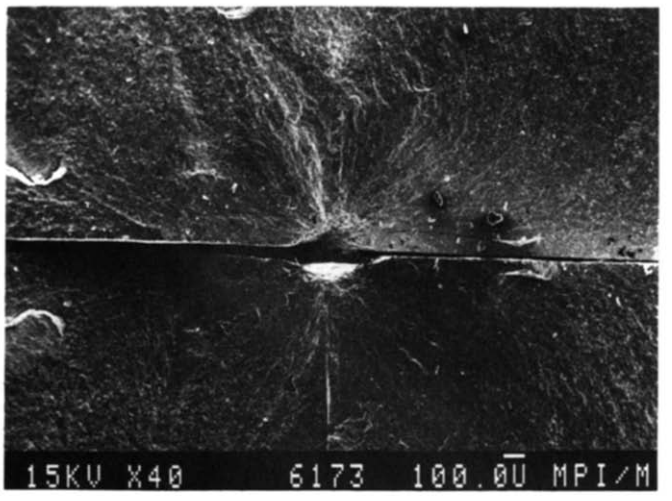

(a)

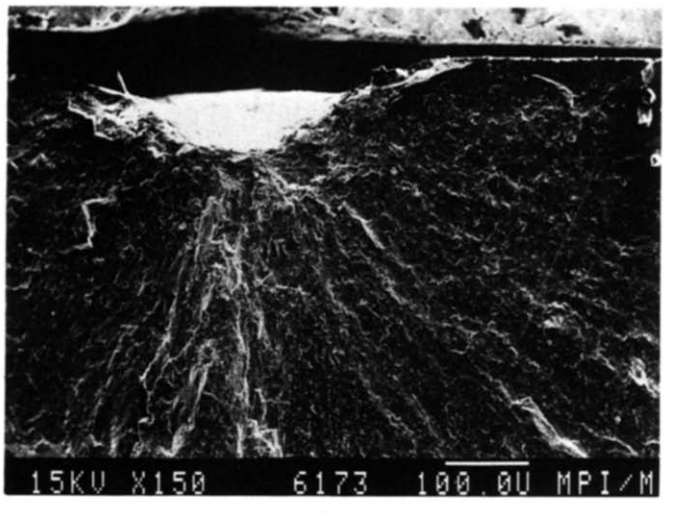

(b)

Fig. 4. Post-indentation fracture surfaces (specimen 8, $P = 392$ N). (a) Both halves of the specimen, median and lateral cracks, (b) lateral cracks.

its influence on the stress distribution in the bending bar was neglected.

Both halves of the broken specimens were put together, indented surfaces face to face, and then the fracture surfaces were photographed in the SEM at different magnifications perpendicular to the fracture surface and under a tilt angle of 20° (see Fig. 3(a) and (b)). From these photographs the lengths and the shape of the radial/median and the lateral crack systems were evaluated (see Fig. 3(a) and (b); Fig. 4(a) and (b)).

Additionally, three-point bending tests with notched specimens of a length of 35 mm and at a span of 30 mm were performed. The tests were run at a constant displacement rate of 0·23 μm/min. From the fracture load P_{max} in the load–displacement curves, K_{max} values were calculated by

$$K_{max} = \sigma_{max}\sqrt{a}\,Y(a/W)$$

with

$$\sigma_{max} = \frac{3}{2}\frac{P_{max}S}{BW^2} \tag{4}$$

where a is the notch depth; W specimen height; B specimen breadth; S span width and $Y(a/W)$ geometrical factor.[6]

3 Results of SEM Investigations of Indentation Bending Tests

The results for the batch of specimens 2–10 are summarized in Table 1. The indenter loads are given in the second column. The diagonals of the impression of the indenter ($2a$) and the lateral crack lengths (c) are given in columns three and four. The evaluation was difficult, because the surface preparation was only down to 6 μm, and therefore the surface patterns were hard to evaluate especially for the low indenter loads. An error of 15% should be admitted for these values.

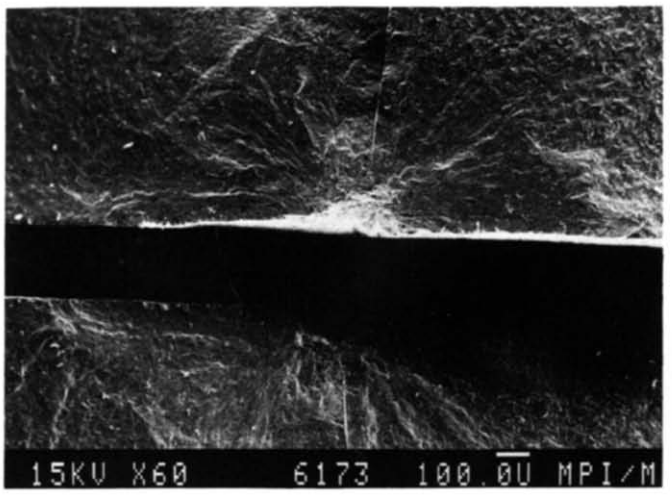

Fig. 5. Post-indentation fracture surfaces, multiple lateral cracks (specimen 9, $P = 490$ N).

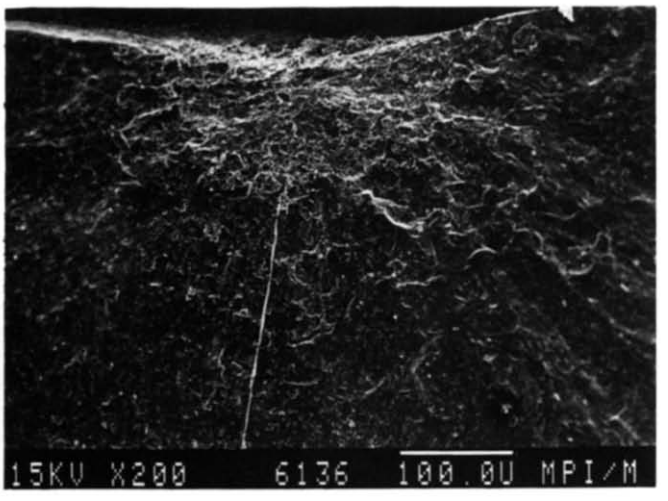

Fig. 6. Post-indentation fracture surface, median and lateral cracks, crushing beneath the indenter (specimen 7, $P = 294$ N).

In general the lateral cracks developed approximately to the same lengths as the radial cracks, for the low loads in direction down into the material (see Fig. 3(a)) then parallel to the surface and for the high loads they turned upwards towards the surface (see Fig. 4(a)). This resulted in part chipping from the surface for specimens 6–10 (see Fig. 2). At the highest indentation loads, for specimens 9 and 10, multiple lateral crack systems developed (see Fig. 5). It could be seen from the SEM pictures that directly beneath the indenter the material was crushed (see Figs 2, 3(a) and 6). This was to be expected, as the material is porous (see Fig. 3(a)).

By means of eqn (1) and the lengths of the diagonals $2a$ (column 3 in Table 1) hardness values were calculated (column 5 in Table 1). The mean value is $H = 8{\cdot}43 \pm 0{\cdot}64$ GPa. K_c values, calculated by the ICL method, eqn (2) in the standardized form, are given in column 6, the mean value being $K_c = 1{\cdot}52 \pm 0{\cdot}08$ MPa$\sqrt{\text{m}}$. Both hardness and K_c are low for a zirconia material, but could be expected because of the porosity of the material.

The K_c values were compared to values K_{max} measured in bending tests with notched specimens, calculated from fracture load P_{max} in the load–displacement curve, Table 2. The result $K_{max} = 1{\cdot}57 \pm 0{\cdot}09$ MPa$\sqrt{\text{m}}$ is in good agreement with the value from the ICL method above.

The bending strengths, measured by breaking the indented specimen (see Table 3, column 3) were used to calculate K_c values by the ISB method, eqn (3). For E in the factor $(E/H)^{1/8}$ in eqn (3) 200 GPa was

Table 2. K_{max} from three point bending with notched specimens (notch width $\sim 60\,\mu$m)

Specimens *Sp*	*Breadth* *B* (*mm*)	*Width* *W* (*mm*)	*Notch depth* *a* (*mm*)	*Fracture load* P_{max} (*N*)	*Stress intensity* K_{max} (*MPa*$\sqrt{m}$)
1B2	1·512	6·942	4·423	10·8	1·62
2B2	1·566	7·012	4·496	10·2	1·48
A1	2·886	6·814	4·332	20	1·61
Mean value					$1{\cdot}57 \pm 0{\cdot}09$

Table 3. Bending strength after Vickers indentations and K_c values from the ISB method for different loads

Specimen *Sp*	*Load* *P* (*N*)	*Fracture stress* σ (*MPa*)	*Factor in eqn (3)* $\sigma P^{1/3}$ (*MPa N*$^{1/3}$)	K_c *from eqn (3)* K_c (*MPa*$\sqrt{m}$)
2	29·4	124·8	384·8	2·4
3	49	(77·1)	—	—
4	98	82·7	380·7	2·4
5	153·1	82·6	441·1	2·7
6	196	80·9	469·1	2·8
7	294	75·3	499·8	2·9
8	392	69·4	506·9	3·0
9	490	69·0	542·9	3·1
10	612·5	63·0	533·9	3·1

chosen, a value that is surely too high for a zirconia material of that porosity. However, this value has only a small influence, because it is taken to the power 1/8. The terms $\sigma P^{1/3}$ should be constant.[5] It can be seen from Table 3, column 4 that the values are not constant but increasing. Thus, the K_c values in Table 3, column 5 show a tendency to increase with the indenter load. Besides, the values exceed those evaluated from the ICL and the displacement controlled bending tests.

There may be two reasons for this disagreement:

—First it is presumed for the evaluation by eqn (3) that η_V^R is invariant when the crack patterns develop geometrically in a well behaved manner. In solids with relatively open structures (e.g. high porosity) the material tends to densify underneath the indenter.[4] For the material investigated crushing was observed. That means that $\eta_V^R = 0{\cdot}59$ as used here from Ref. 5 may not be the appropriate value.

—Second the bending-strength values themselves may be overestimated because the radial/median cracks, which cause fracture, are screened by the lateral cracks perpendicular to them.

4 On the Relation between Impedance Spectroscopy Results and the Development of the Crack Systems

The original goal of this investigation was to find a correlation between impedance spectroscopy results and microcracks in ceramic materials. To discuss this correlation it is important to mention that the pin-shaped measuring electrode for the impedance measurements was positioned on one of the symmetry axes of the indentation pattern at a distance of 250 μm from one of the corners of the pattern. With the impedance spectroscopic investigation in Ref. 1 two regions were distinguished: a 'low load domain' up to specimen 4 and a 'high load domain' from specimens 5–10.

—The intragrain resistance R_{ig} and consistently the intragrain capacity C_{ig}, characterizing the average dielectric properties of the bulk material, vary only a little and thus remain nearly unaffected by the indentation pattern.

—The internal surface (intergrain) resistance R_s and consistently the capacity C_s, proportional to the surface of the grain boundaries, vary with the indentation patterns and with the load.

These facts may be interpreted as follows:

—In the 'low load domain' both R_s and C_s decrease with the load to a minimum. In this region the position of the pin electrode was outside the range of the lateral cracks (see Table 1). This means that the lateral cracks, which are approximately parallel to the specimen surface and thus perpendicular to the direction of the current from the pin-electrode have a small influence on R_s and C_s. The only influence may result from the densification of the material by crushing it in and around the indenter pattern, resulting in a better contact between the grains and thus lowering of R_s and C_s. This is consistent with the decrease of the 'blocking factor' $\alpha = R_s/R_t$ in this region.[1]

—In the 'high load domain', from specimens 5–10 the lateral cracks spread beneath the pin electrode, the intergrain resistance rises and thus do R_s, C_s and simultaneously the blocking factor α.

—The variation in the depression angles β_{ig} and β_s, the characteristic factors for the homogeneity, seems consistent with this interpretation: β_{ig} remains unaffected, while β_s falls in the 'low load domain'—the homogeneity is improved. Then in the 'high load domain' the homogeneity is disturbed by the lateral cracks, β_s increases to reach a new kind of homogeneity, influenced by lateral cracks only. β_s falls again from specimens 8–10.[1] Perhaps this fact is consistent with the appearance of multiple lateral cracks for specimens 9 and 10.

5 Summary and Outlook

The goal of the investigation was to find a correlation between microcracks and impedance spectroscopy parameters to promote impedance spectroscopy as a tool for non-destructive testing of ceramics.

Relatively well defined damage was introduced into YSZ-zirconia, a model material for an ionically conducting ceramic material, by indentation technique.

First the evaluation of stress intensity factors K_c from hardness indentations to characterize the material was discussed and the ICL (indentation crack length) and ISB (indentation strength in bending) methods were compared. The ICL method proved to give relevant results.

SEM investigations proved that the impedance spectroscopy parameters R_{ig} (intragrain resistance) and C_{ig} (intragrain capacity), R_s (internal surface resistance) and C_s (intergrain surface capacity), α (blocking factor) and β (homogeneity coefficient) correlate with the damage introduced to the material by indentation. R_s, C_s and α could be

regarded directly as parameters characterizing the development of microcracks in the zirconia material.

Acknowledgement

This work was supported by the Commission of the European Communities under contract number MA1E-0066.

References

1 Dessemond, L. & Kleitz, M., Effects of mechanical damage on the electrical properties of zirconia ceramics. *J. Europ. Ceram. Soc.*, **9** (1992) 35–9.

2. Lawn, B. R. & Marshall, D. B., Hardness, toughness and brittleness: an indentation analysis. *J. Am. Ceram. Soc.*, **62** (1979) 347–50.
3. Ponton, C. B. & Rawlings, R. D., Vickers indentation fracture toughness test, Part 1: Review of literature and formulation of standardised indentation toughness equation. *Mater. Sci. and Techn.*, **5** (1989) 865–72.
4. Anstis, G. R., Chantikul, P., Lawn, B. R. & Marshall, D. B., A critical evaluation of indentation techniques for measuring toughness: I. Direct crack measurements. *J. Am. Ceram. Soc.*, **64** (1981) 533–8.
5. Anstis, G. R., Chantikul, P., Lawn, B. R. & Marshall, D. B., A critical evaluation of indentation techniques for measuring toughness: II. Strength method. *J. Am. Ceram. Soc.*, **64** (1981) 539–43.
6. Srawley, J. E., Wide range stress intensity factor expressions for ASTM E 399 standard fracture toughness specimens. *Int. J. Frac. Mech.*, **12** (1976) 475–6.